

## RESEARCH PAPER

## RESEARCH OF PHYSICO-CHEMICAL PROPERTIES OF FERROUS SANDS FROM ALUMINA PRODUCTION

Aigul Zhunusova<sup>1</sup>, Ablay Zhunusov<sup>1\*</sup>, Petr Bykov<sup>1</sup>, Altynsary Bakirov<sup>1</sup>, Oleg Zayakin<sup>2</sup>, Anar Kenzhebekova<sup>1</sup><sup>1</sup>Toraighyrov University, Lomov st. 64, Pavlodar city, Kazakhstan<sup>2</sup>Institute of Metallurgy of the Ural Branch of the Russian Academy of Sciences, Amundsen st. 101, Yekaterinburg city, Russia

\*Corresponding author: zhunusov\_ab@mail.ru, tel.: +77478086235, Department of Metallurgy, Faculty of Engineering, Toraighyrov University, 140008, St. Ak. Chokina 139, Pavlodar city, Kazakhstan

Received: 23.10.2024

Accepted: 16.11.2024

## ABSTRACT

This research is devoted to sintering ferruginous sand – waste from alumina production. The research allowed us to determine the optimal process parameters for obtaining iron ore and fluxed agglomerate. When studying the effect of flux additives in the composition of the agglomeration batch, we considered them from the position of multicomponent oxide systems based on the phase diagrams of the FeO-CaO-Fe<sub>2</sub>O<sub>3</sub>-Al<sub>2</sub>O<sub>3</sub>, FeO-MgO-Fe<sub>2</sub>O<sub>3</sub>-Al<sub>2</sub>O<sub>3</sub> and FeO-MgO-CaO-Fe<sub>2</sub>O<sub>3</sub> systems. The thermal transformations in the ferruginous sands and the agglomerate obtained from them were studied. The obtained derivatograms indicate the complexity of the mineral composition of the iron ore materials under study. According to the X-ray phase analysis, wustite FeO and magnetite Fe<sub>3</sub>O<sub>4</sub> are recorded during agglomeration. Also, X-ray phase analysis reveals the appearance of hercynite FeAl<sub>2</sub>O<sub>4</sub>. It provides recommendations for avoiding undesirable factors of the formation of low-melting phases from the position of the oxide system FeO-MgO-CaO-Fe<sub>2</sub>O<sub>3</sub>. The presented X-ray phase and petrographic studies confirm the study's results.

**Keywords:** Agglomeration; sintering; ferrous sand; iron ore agglomerate; fluxes

## INTRODUCTION

In Kazakhstan, as in some countries, there is an acute problem of technogenic waste disposal. At the enterprises of Kazakhstan, a large amount of waste sludge is formed, including waste from energy companies and non-ferrous and ferrous metallurgy plants [1, 2]. Only at JSC "Aluminium of Kazakhstan" about two million tons of waste sludge accumulate in waste dumps per year. Much waste sludge is considered substandard and used only in highway construction as bulk material. Iron oxide (Fe<sub>2</sub>O<sub>3</sub>) reaches 15-20% in the waste sludge composition. At JSC, "AK" alumina is obtained from bauxites from Kazakhstan deposits. As is known, bauxites of Kazakhstan deposits are distinguished by a large amount of iron and silicon [3]. Therefore, the leaching method isolates ferrous sands with a Fe<sub>2</sub>O<sub>3</sub> content of 50-65% at the first stage of bauxite processing. These ferrous sands are sent to sludge fields according to the general scheme and do not find further use. As a result, together with the remains of red and gray sludge, ferrous sands lose their value as iron ore material, mixing with other sludges. For ferrous metallurgy, the iron oxide content in iron ore of 50-65% is considered rich ore and is used in the production of cast iron in blast furnaces. These wastes (ferrous sands) are suitable not for sending them to sludge fields, but for further use in metallurgical production. Naturally, considering these wastes' physical and chemical characteristics with the correct selection of processing technology and involving waste in metallurgical processing. It should also be considered that these wastes can be an additional source of raw materials for producing ferrous metals (cast iron, ferrosilicon) for many years. Over 50 million tons of bauxite waste have accumulated in sludge fields. Regarding iron oxide, approximately 10 million tons have already been irretrievably lost. Considering the iron content in ferrous sands, a substandard material sent to the sludge field in approximately 300 thousand tons per year is only in Kazakhstan. According to [4], over 2.7 billion tons of alumina production waste have accumulated worldwide, increasing by 120 million tons annually.

Various works on the processing of alumina production waste are presented worldwide. However, not all of the studies conducted are of interest from the metallurgy side. Many technologies for processing alumina production waste are distinguished by the high cost of implementing the presented studies, and most of them are accompanied by complexity and multi-stage processing. Because of its composition, bauxite waste can be used in various industries [5,6,7].

The works [8,9,10] present various options for using alumina production waste in various industries. The presented studies consider technologies for using construction waste as cements, catalysts for processing waste oil, hydrometallurgical, pyrometallurgical methods and direct use of alumina production sludge. Also, much attention is paid to the recycling and use of other

iron-containing man-made waste in metallurgical processing [11]. Almost all waste generated at metallurgical plants in foreign countries is used in agglomeration and other industries [12,13,14,15]. Thus, for the economy of Kazakhstan, the development of technology for processing ferrous sands plays a huge role, since hundreds of thousands of tons of waste end up in sludge dumps yearly. In terms of years of work of JSC "AK" and an irrational approach to such high-quality material, it amounts to tens of millions of tons of waste containing a large amount of iron and turned out to be unusable. However, there is still time. By developing rational technology in the form of an agglomeration method and obtaining high-quality iron ore agglomerate with an iron content of over 50%, up to 30% of natural iron ore is saved.

## MATERIAL AND METHODS

## Raw materials

To work with ferruginous sands – bauxite waste, samples were taken at JSC Aluminium of Kazakhstan to obtain iron ore and fluxed agglomerate in laboratory conditions. The disadvantages of ferruginous sands include high humidity (up to 50%) and non-compliance of the granulometric composition (**Table 1**) with the pelletizing requirements. However, pelletizing accelerates with an increase in the number of embryos in charge, namely with an increase in the amount of return and granular ores. From the theory of pelletizing [16], it is known that the most unfavorable effect on pelletizing is exerted by the fraction of 0.1 - 1.6 mm. From **Table 1** the studied ferruginous sands – bauxite waste fall into this size range. The 0.2 - 1.0 mm fraction represents the main fraction of ferruginous sands, more than 60% (63.7%). **Table 1** shows that ferrous sand does not have a fine fraction in its composition, mainly represented by large pieces. To improve the conditions for pelletizing ferrous sand, a finely dispersed material, aspiration dust, was used. Aspiration dust is formed due to the operation of metallurgical units (furnaces, crushers, etc.) and is captured by the aspiration systems of the workshops. Such material is also considered substandard waste and requires disposal.

**Table 1** Granulometric composition of ferruginous sands

Fraction, mm	-0.06	-0.2-0.06	-0.5-0.2	-1-0.5	-3-1	-5-3
Units of m. %	2.0	14.7	43.2	20.5	6.8	12.8

Before pelletizing, ferrous sand was pre-dried at 100-150 °C in a drying oven, since this material has a high moisture content (up to 40%) when separated from bauxite. The material moisture content was reduced to 15-20%. The following

were used as an agglomeration batch: waste sludge (10%), aspiration dust (20%), coke breeze (5%), return (20%), fluxes (10% magnesium oxide and 10% calcium oxide), the rest was ferrous sand. Mixing and pelletizing were carried out in a drum mixer. For better pelletizing of ferrous sand, aspiration dust of 0-1 mm fraction was used in the mixture. The degree of pelletizing of the studied material is improved due to clay particles in the aspiration dust. Coke screenings were used as fuel (Table 2).

**Table 2** Chemical and technical composition of coke ash, %

SiO <sub>2</sub>	CaO	MgO	Al <sub>2</sub> O <sub>3</sub>	Fe <sub>2</sub> O <sub>3</sub>	A	V	W
40.3	11	6.7	10.2	11.7	26.1	6.1	8.0

Laboratory studies were carried out according to the methodology adopted in the university laboratory [17]. Bowl parameters: diameter 100 mm, bowl height allows batch sintering up to 500 mm. The agglomeration unit is equipped with a vacuum pump VVN-1.5, thermocouples TXA, VR and an automatic multichannel temperature recorder (AMRT-6) simultaneously recording the gas outlet's temperature and the sintered batch's layer. Laboratory sintering of ferrous sands established the following: vertical sintering speed - 19.0 mm/min; specific productivity - 0.91 t / m<sup>2</sup> h; drum impact strength - 79.9%; temperature in the layer - 1340 °C.

**Fig. 1** shows photographs of ferrous sand - waste from alumina production and the resulting iron ore agglomerate.

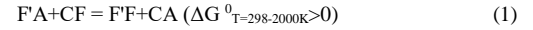


**Fig. 1** Ferrous sand (a) and iron ore agglomerate (b)

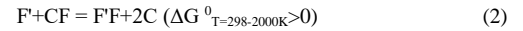
According to [18], microscopic and X-ray phase analyses of the synthesis products indicated a single-phase nature of the obtained samples, thereby confirming some phases, in particular hercynite (FeAl<sub>2</sub>O<sub>4</sub>) in the four-component FeO-CaO-Fe<sub>2</sub>O<sub>3</sub>-Al<sub>2</sub>O<sub>3</sub> system. Hercynite, according to its temperature characteristics (softening and melting temperatures), belongs to low-melting ones. This iron compound is low-melting and has very high electrical conductivity. Therefore, the process of melting an agglomerate of ferrous sands can be accompanied by the formation of low-melting slags, i.e. the rate of slag formation is higher than the iron reduction rate. This leads to a breakdown in the operation of the furnace, unless special measures are taken to prevent the indicated negative factors. If these movements are carried out near spinel planes (iron monoaluminate, magnesia spinel, ferrite spinel), the slags formed in this case will be more refractory. To prevent undesirable processes of formation of low-melting slags, it is necessary to use fluxing materials based on magnesium oxide or calcium oxide that are already in the agglomeration of ferruginous sands. However, magnesium oxide reduces the hercynite in the agglomerate but does not move the structure to another area. The use of calcium oxide allows you to move the structure to other areas, with the formation of more refractory compounds. Using agglomerate fluxed with calcium oxide in cast iron smelting can ensure the formation of more refractory final slags. But in this case, it is necessary to identify the nature of the change in the phase composition of the agglomerates and the resulting slags and, accordingly, their properties, depending on the number of fluxes used in the charge. In this regard, it is necessary to study the effect of flux additives in the composition of the agglomeration batch from the position of the state diagrams of the FeO-CaO-Fe<sub>2</sub>O<sub>3</sub>-Al<sub>2</sub>O<sub>3</sub>, FeO-MgO-Fe<sub>2</sub>O<sub>3</sub>-Al<sub>2</sub>O<sub>3</sub> and FeO-MgO-CaO-Fe<sub>2</sub>O<sub>3</sub> systems. Using multicomponent oxide systems helps interpret chemical interactions in complex systems, thereby facilitating the development and optimization of technological processes [19, 20].

**Study of iron ore materials from the position of multicomponent oxide systems.**

In the FeO-CaO-Fe<sub>2</sub>O<sub>3</sub>-Al<sub>2</sub>O<sub>3</sub> system (Figure 2 a) there is a reciprocal system, as in the magnesia system (Fe<sup>2+</sup>, Ca<sup>2+</sup>// Fe<sub>2</sub>O<sub>4</sub><sup>2-</sup>, Al<sub>2</sub>O<sub>4</sub><sup>2-</sup>) with the main diagonal F'A (hercynite) – CF (calcium monoferrite) following ΔG<sub>T</sub><sup>0</sup> by the reaction:



In addition, the presence of a stable line F'-C<sub>2</sub>F according to the reaction:



changes the phase diagram of this system (Figure 2 a). At the same time, due to these two binary subsystems, three quasi-ternary subsystems F'-F'A-C<sub>2</sub>F, F'A-C<sub>2</sub>F-CF, F'A-CF-A appear inside the tetrahedron, which cut off all calcium aluminates from magnetite (FF), which is clearly shown in the parts of the F'-C-F-A system moved apart from each other relative to the mutual system Fe<sup>2+</sup>, Ca<sup>2+</sup>// Fe<sub>2</sub>O<sub>4</sub><sup>2-</sup>, Al<sub>2</sub>O<sub>4</sub><sup>2-</sup>. According to the data of [21], the processes of interaction of the components of the iron ore charge with fluxing materials proceed mainly with the formation of low-melting melts near calcium ferrites, which are mixtures with magnetite, wustite, hercynite and calcium monoaluminate.

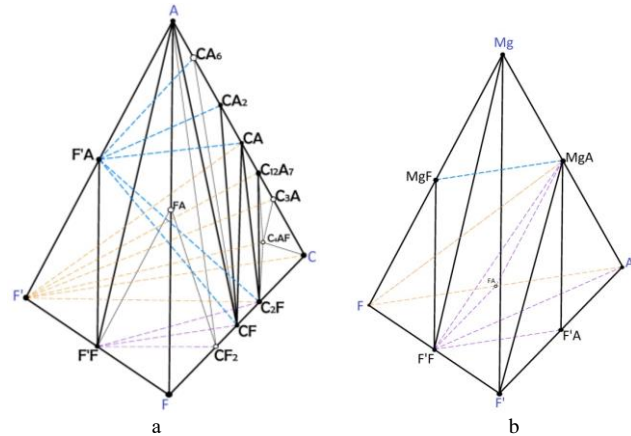
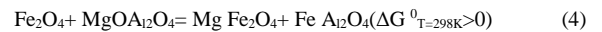
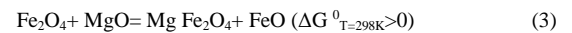


**Fig. 2** Phase structure diagram of the system: a - F'-C-F-A; b - F'-Mg-F-A

The appearance of calcium aluminates as an independent phase is possible upon completion of all reactions in mixtures with the achievement of equilibrium mainly in the high-calcium or magnesia parts of the system. However, the X-ray phase analysis of the agglomerate obtained from ferruginous sand shown in Figure 4 did not reveal the formation of calcium monoaluminate. The lines of accompanying phases presented in Table 3 for each congruently melting phase of the system can be used to identify stable polytopes of the general six-component system F-C-Mg-F-A-S. From Table 3, the presence of greinitzite in the C-Mg-F-A system is also observed.

In the FeO-MgO-Fe<sub>2</sub>O<sub>3</sub>-Al<sub>2</sub>O<sub>3</sub> (F'-Mg-F-A) system (Figure 2 b), the determining reactions in the system are:



Which divides the lateral sides of the tetrahedron into six stable quasi-quaternary subsystems with the presence of a mutual system Fe<sup>2+</sup>, Mg<sup>2+</sup>// Fe<sub>2</sub>O<sub>4</sub><sup>2-</sup>, Al<sub>2</sub>O<sub>4</sub><sup>2-</sup> with the main diagonal Fe<sub>3</sub>O<sub>4</sub>-MgAl<sub>2</sub>O<sub>4</sub>, arising from the second reaction (Table 4).

**Table 3** Coexisting phases of the C-Mg-F-A system

№	Phase	Abbreviated formula	Coexisting phase
1	Wustit	F'	F'F, C <sub>2</sub> F, C, (C <sub>4</sub> AF), (C <sub>3</sub> A), C <sub>12</sub> A <sub>7</sub> , CA, FA
2	Alumina	A	F'A, FF, (FA), (F), (CF <sub>2</sub> ), CF, (CA <sub>6</sub> ), CA <sub>2</sub>
3	Hematite	(F)	F'F, (FA), A, (CF <sub>2</sub> ), CF
4	Lime	C	C <sub>2</sub> F, (C <sub>4</sub> AF), (CA <sub>3</sub> ), C <sub>12</sub> A <sub>7</sub> , F'

5	Magnetite	FF	F',(F),(FA),A, F'A,(CF <sub>2</sub> ), CF, C <sub>2</sub> F
6	Monocalcium ferrite	CF	(F),(C <sub>2</sub> F), FF, F'A,A,(CA <sub>6</sub> ), CA <sub>2</sub> ,CA, C <sub>2</sub> F
7	Dicalcium ferrite	C <sub>2</sub> F	CF, FF, F, F'A,A,(CA <sub>6</sub> ),CA <sub>2</sub> ,CA, C <sub>2</sub> F
8	Twelve-calcium semialuminate	C <sub>12</sub> A <sub>7</sub>	CF, FF, F, F'A,CA, C <sub>12</sub> A <sub>7</sub> , (C <sub>4</sub> AF),C
9	Calcium monoaluminate	CA	C <sub>12</sub> A <sub>7</sub> , C <sub>2</sub> F, CF, F, F'A, CA <sub>2</sub>
10	Calcium dialuminate	CA <sub>2</sub>	CA,CF, F'A,(CA <sub>6</sub> ),A
11	Hercynite	F'A	F', FF, CF, C <sub>2</sub> F,CA, CA <sub>2</sub> ,(CA <sub>6</sub> ),A

**Table 4** Coexisting phases of the system F'-Mg-F-A

N <sub>o</sub>	Phase	Abbreviated formula	Coexisting phase
1	Wustit	F'	F'F, F'A, Mg, MgA
2	Alumina	A	F'A, FF,( FA),( F), MgA
3	Hematite	(F)	F'F,MgF, MgA,(FA), A
4	Magnesia	Mg	MgF, F'F, F', MgA
5	Magnetite	F'F	( F), F', MgF, MgA,(FA), A,F'A
6	Iron monoaluminate	F'A	F',F'F, MgA,A
7	Magnesian spinel	MgA	A, F'A, F', F'F, (F),MgF,Mg, (FA)
8	Ferritic spinel	MgF	(F),F'F,MgA, Mg

**Table 4** and **Fig. 2 (b)** show the presence of hercynite in the F'-Mg-F-A system. With the introduction of magnesium oxide into the batch composition during the agglomeration of ferrous sand, the amount of hercynite will decrease with the formation of new phases. More refractory phases of iron monoaluminate, magnesia and ferrite spinels are observed.

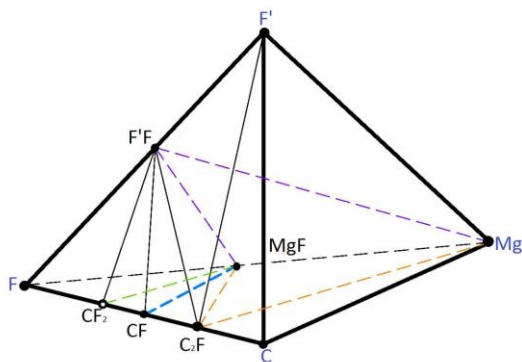


**Fig. 3** Phase structure diagram of the system F'-Mg-C-F

In the presented diagram (**Fig. 3**) of the F'-Mg-C-F system, the presence of hercynite is not observed for the coexisting phases. According to this diagram, it is theoretically possible to avoid undesirable processes of low-melting slag formation, as noted above. To avoid the formation of low-melting slags, fluxing materials are necessary. The most suitable flux is calcium oxide. Using calcium oxide will allow the structure to be moved to other areas and form more refractory compounds. In the future, agglomerate fluxed with calcium oxide in cast iron smelting will ensure the formation of more refractory final slags. To reduce energy costs, smelting ferrous metals and alloys (ferrosilicon) should be carried out on pre-prepared raw materials, using these materials with fluxing additives and a modified composition of ferrous sand with a minimum content of low-melting compounds. Therefore, to select the optimal composition of the agglomeration charge with the addition of fluxes, it is necessary to analyze the

physical and chemical properties and ways of optimizing the composition of iron ore materials intended for smelting ferrous metals and alloys.

**RESULTS AND DISCUSSION**

**Study of metallurgical properties of iron ore materials**

The metallurgical properties of iron ore materials, especially ferruginous sands – waste from alumina production- differ significantly and depend on the iron amount, their structure and chemical composition, and the ratio of iron oxides in the ore. The chemical composition of ferruginous sands, iron ore and fluxed agglomerates are given in **Table 5** and **Table 6**.

**Table 5** Chemical composition of the studied samples of ferruginous sands – waste from alumina production

Sample No.v	Material	Fe <sub>2</sub> O <sub>3</sub>	SiO <sub>2</sub>	Al <sub>2</sub> O <sub>3</sub>	CaO	MgO	S
1	Ferrous sand is a waste product of alumina production	55.9	7.8	19.1	5.70	1.62	0.20

**Table 6** Chemical composition of iron ore and fluxed agglomerates

Sample No.	Material	Fe <sub>gen</sub>	FeO	SiO <sub>2</sub>	Al <sub>2</sub> O <sub>3</sub>	CaO	MgO	S
1	Iron ore agglomerate	53.0	28.9	11.3	15.8	4.96	4.86	0.02
2	Magnesium oxide fluxed agglomerate	55.9	16.5	6.50	6.70	7.60	8.90	0.08
3	Calcium oxide fluxed agglomerate	57.6	14.5	6.40	3.70	10.3	2.20	0.04

The host rock is represented by a number of components, the composition and quantity of which also significantly affect the ore properties. An integrated approach to the analysis of ore properties allows us to fully evaluate its metallurgical properties, which is important when studying technogenic waste and using a combination of different ores to form a charge, both for obtaining agglomerate and for smelting ferrous metals.

In this regard, the work included studies of thermal transformations in the studied ferruginous sands and the agglomerate obtained from them.

Differential thermal analysis was carried out in an oxidizing atmosphere of air on a derivatograph. Recording of temperature and differential curves was carried out using a platinum-platinum-rhodium thermocouple. The heating rate was 10 degrees per minute, the tape drawing speed  $v = 2 \text{ mm / min}$ . The sensitivity of the DTA derivatograph was 0.5 mV, DTG - 1.0 mV, TG - 200-500 mg. Samples were placed in a corundum crucible with a diameter of 10 and a height of 12 mm in powder form. The duration of the experiments was 100 minutes. The thermal effects are interpreted using available literature data and the results of X-ray phase studies. In many cases, in addition to individual publications on the thermoanalytical characteristics of minerals, we were guided by summary tables summarizing these data [22,23,24,25,26].

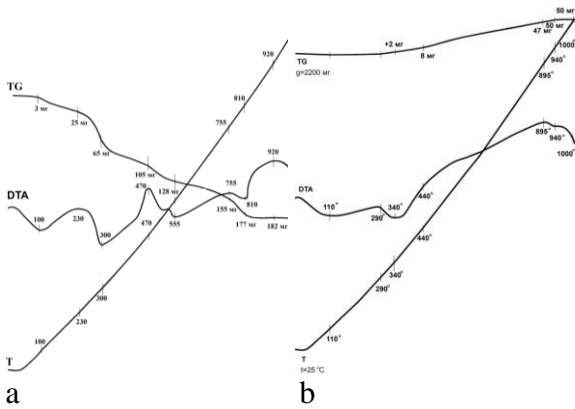


Fig. 4 Derivatograms of ferrous sand (a) and iron ore agglomerate (b)

The derivatogram of ferrous sand, a waste product of alumina production (Fig. 4a), shows four endothermic effects indicating a wide range of physical and chemical transformations. The endothermic effect at 100 °C corresponds to the loss of hygroscopic moisture, and the endothermic decrease in the region of 300 °C indicates the presence of small amounts of lepidocrocite  $\gamma$ -FeO·OH ( $\text{Fe}_2\text{O}_3 \cdot \text{H}_2\text{O}$ ) with a cubic structure in a sample of hematite ( $\alpha$ - $\text{Fe}_2\text{O}_3$ ) with a trigonal structure. During a further increase in temperature at 230 °C, the siderite presents in the ferrous sand, which has a heat capacity of 1.654 kJ/(kg·K), is heated, increasing its physical heat to 470 °C. The data in Fig. 5 confirms the presence of siderite. During this period, their internal structure changes slightly with a gradual increase in the heat content of the samples. In this range, the exothermic effect recorded at 470 °C during the oxidation of  $\text{Fe}_2\text{O}_3$  is also superimposed. At a temperature of 555 °C, the endothermic impact associated with the magnetic transformations of magnetite  $\text{Fe}_3\text{O}_4$  appears. At 755 °C, in the presence of solid carbon, the reduction of iron oxides under oxidizing conditions and the decomposition of dolomite present in ferrous sand and the dissociation of  $\text{MgCO}_3$  begins. At 810 °C,  $\text{Fe}_3\text{O}_4$  is reduced to FeO with the superimposition of the dissociation of  $\text{CaCO}_3$  (44%  $\text{CO}_2$ ).

Analysis of the derivatograms of iron ore agglomerate (Fig. 4 b) allows us to identify some process stages. During heat treatment, the iron ore agglomerate is initially subjected to dehydration processes (at 110 °C) to remove physically bound moisture. During further temperature increase to 290 °C, materials with a heat capacity of 1.654 kJ/(kg·K) are heated with an increase in their physical heat. During this period, their internal structure changes slightly with the gradual increase of the heat content of samples.

The exothermic effect detected at 290 °C relates to the combustion of residual solid carbon in iron ore agglomerate. In the temperature range of 290 - 440 °C (at 340 °C) development of processes of dissociation of iron carbonates is observed with loss of mass and absorption of heat (67.11 kJ/kg). Formed oxides enter into solid-phase reactions with each other with the formation of magnetite-wüstite and magnomagnetite.

Upon reaching the heating level of 440 °C in the air atmosphere, the phenomena of oxidation of the formed compounds to ferrite and hematite with absorption and at 895 °C with release of excess heat develop. In this case, the heat content of the samples increases. At higher temperatures of 940 °C, solid-phase sintering processes of the initial components are observed with the formation of poorly soluble silicates and a decrease in their heat content by 168.4 kJ/kg. A further increase in the heating level of the samples to 1000 °C is accompanied by the reduction of iron oxide forms  $\text{Fe}_3\text{O}_4$  to FeO. From the X-ray diffraction pattern of ferrous sand (Fig. 5), it is evident that along with hematite ( $\text{Fe}_2\text{O}_3$ ), magnetite ( $\text{Fe}_3\text{O}_4$ ), the formation of associated minerals calcite ( $\text{CaCO}_3$ ) and siderite ( $\text{FeCO}_3$ ) is observed. During agglomeration, iron silicates are destroyed under reducing conditions, under which siderite is formed.

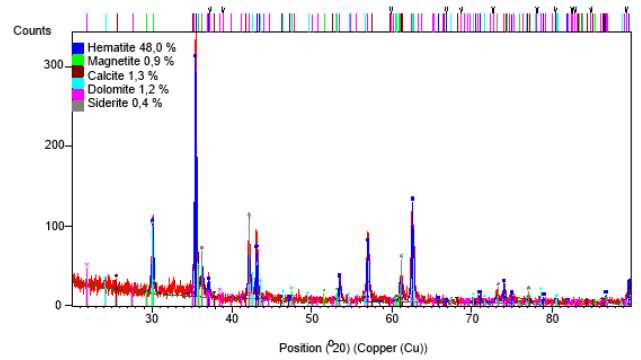


Fig. 5 Radiograph of ferrous sand

Fig. 6 shows the mineralogical composition of the agglomerate according to the qualitative X-ray phase analysis (XPA). According to the XPA data, wüstite FeO and magnetite  $\text{Fe}_3\text{O}_4$  are recorded during agglomeration. X-ray phase analysis also reveals the appearance of hercynite  $\text{FeAl}_2\text{O}_4$ . The appearance of hercynite in the structure of the iron ore agglomerate is confirmed by the petrographic data presented in Figs 9, 10.

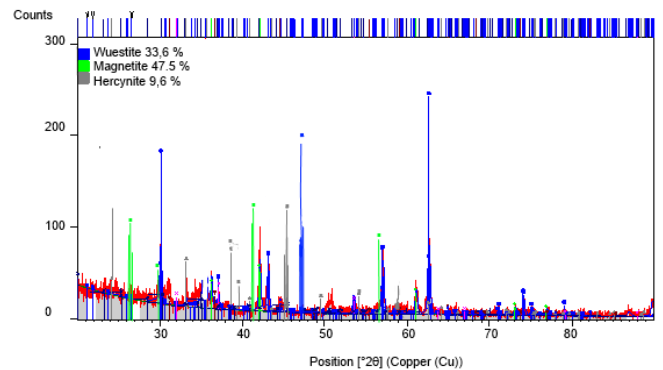


Fig. 6 X-ray diffraction pattern of iron ore agglomerate

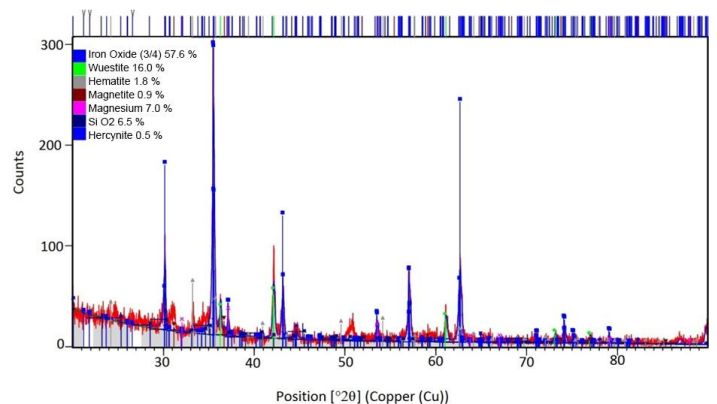
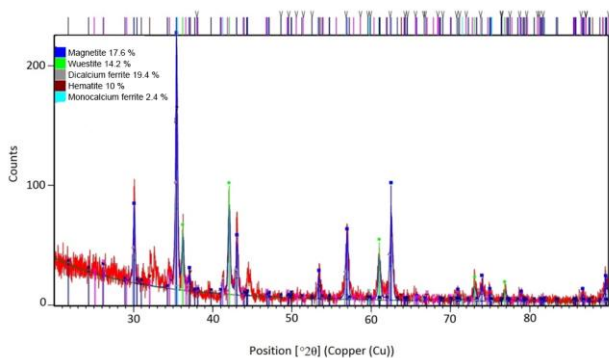


Fig. 7 X-ray diffraction pattern of magnesium oxide fluxed agglomerate

From the given XRD data (Fig. 7), during sintering of magnesium oxide-fluxed magnesium, wüstite FeO, magnetite  $\text{Fe}_3\text{O}_4$ , hematite  $\text{Fe}_2\text{O}_3$ , silica, magnesia is recorded, and gretznite  $\text{FeAl}_2\text{O}_4$  is also present in small quantities. From Fig.8, when calcium oxide is introduced as a flux during the sintering of ferrous sand, new minerals of dicalcium ferrite and monocalcium ferrite are detected.



**Fig. 8** X-ray diffraction pattern of calcium oxide fluxed agglomerate

To confirm the presence of hercynite in the samples studied of iron ore and fluxed agglomerate, a sample (Figs. 9, 10) with pieces ranging in size from 0.5 to 2.5 cm was examined using an Olympus BX51 microscope. The texture of the sample is loose, multi-porous, and strong. The colour is grey to black; the lustre is matte, and metallic in places. The structure is fine-grained. According to X-ray phase analysis, the sample is represented by magnetite, wustite, and hercynite (Fig. 5).

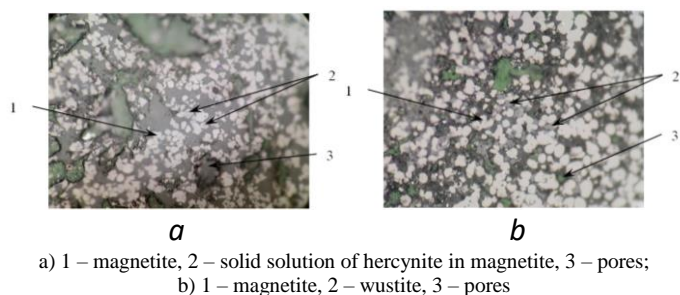
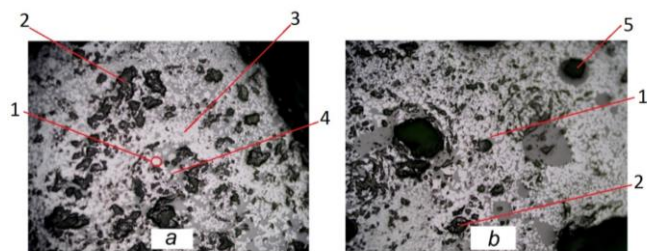


**Fig. 9** Fragment of the microstructure of iron ore agglomerate, x500

In Fig. 10, the fragment of the agglomerate's microstructure shows magnetite, a solid solution of hercynite in magnetite and wustite. In Fig. 10 (b), hercynite is not observed, which confirms the theory of using fluxes in agglomeration. The most suitable flux for the agglomeration of ferruginous sands is calcium oxide.



1 – Magnetite; 2 – Wustite; 3 – Magnesia; 4 – Hercynite; 5 – Pores

**Fig. 10** General view of the microstructure of fluxed agglomerate (a – magnesium oxide, b – calcium oxide) x100

## Conclusions

The conducted studies show that hercynite is detected during the agglomeration of ferruginous sands – waste from bauxite processing. The appearance of solid solutions of hercynite in magnetite in the agglomerate is explained by the fact

that magnetite is the first to crystallize from the iron-silicate melt, which absorbs alumina from the melt. Magnetite-hercynite has extremely poor reducibility. The presence of aluminum ions in the system significantly increases the temperature of the reduction onset. Thus, the initial raw material with 10% hercynite in magnetite is reduced at 1000 °C. The formation of hercynite during agglomeration in the process of melting the agglomerate is accompanied by the formation of low-melting slags, i.e. the rate of slag formation is greater than the iron reduction rate. This leads to a breakdown in the furnace operation unless special measures are taken to prevent the above-mentioned negative factors. If these movements are carried out near spinel planes (iron monoaluminate, magnesia spinel, ferritic spinel), the resulting slags will be more refractory. To obtain high-quality agglomerated material and use it in the production of cast iron or silicon ferroalloys, the work investigated the physicochemical properties and possible phase transformations occurring during heat treatment of ferrous sands based on multicomponent oxide systems FeO-CaO-Fe<sub>2</sub>O<sub>3</sub>-Al<sub>2</sub>O<sub>3</sub>, FeO-MgO-Fe<sub>2</sub>O<sub>3</sub>-Al<sub>2</sub>O<sub>3</sub> and FeO-MgO-CaO-Fe<sub>2</sub>O<sub>3</sub>. When introducing calcium oxide into the agglomeration batch, new minerals of dicalcium ferrite and monocalcium ferrite are detected. Thus, the F-Mg-C-F system diagram data confirms the possible absence of hercynite. According to this diagram, it was theoretically assumed that undesirable formation processes of low-melting slags should be avoided. To prevent the formation of low-melting slags, it is necessary to use fluxing materials, such as calcium oxide, as shown by X-ray phase studies. Using calcium oxide at the agglomeration stage will allow the structure to move to other areas and form more refractory compounds. In the future, agglomerate fluxed with calcium oxide in the smelting of cast iron or silicon ferroalloys will ensure the formation of more refractory final slags.

**Acknowledgements:** The authors are grateful for the support of experimental works by a project funded by the Science Committee of the Ministry of Science and Higher Education of the Republic of Kazakhstan (grant AR 23488812).

## REFERENCES

1. A. Bakirov, S. Abdulina, A. Zhunusov, N. Oleinikova: Chemical Engineering Transactions, 88, 2021, 973–978. <https://doi.org/10.3303/CET2188162>.
2. P. Bykov, A. Kuandykov, A. Zhunusov: Defect and Diffusion Forum, 410, 2021, 405–410. <https://doi.org/10.4028/www.scientific.net/ddf.410.405>.
3. A.T. Ibragimov, S.V. Budon: *Development of technology for producing alumina from bauxites of Kazakhstan*. Pavlodar: LLC Dom Pechati, 2010, 304 p.
4. G. Power, M. Grafe, C. Klauber: Hydrometallurgy, 108(1-2), 2011, 33–45. <https://doi.org/10.1016/j.hydromet.2011.02.006>.
5. C. Klauber, M. Grafe, G. Power: Hydrometallurgy, 108(1-2), 2011, 11–32. <https://doi.org/10.1016/j.hydromet.2011.02.006>.
6. M. Grafe, G. Power, C. Klauber: Hydrometallurgy, 108(1–2), 2011, 60–79. <https://doi.org/10.1016/j.hydromet.2011.02.004>.
7. M. Grafe, C. Klauber: Hydrometallurgy, 108(1-2), 2011, 46–59. <https://doi.org/10.1016/j.hydromet.2011.02.005>.
8. P.E. Tsakiridis, S. Agatzini-Leonardou, P. Oustadakis: Journal of Hazardous Materials, 116(1-2), 2004, 103–110. <https://doi.org/10.1016/j.jhazmat.2004.08.002>.
9. A.I. Cakici, J. Yanik, S.U.T. Karayildirim, H. Anil: Journal of Material Cycles and Waste Management, 6(1), 2004, 20–26. <https://doi.org/10.1007/s10163-003-0101-y>.
10. M.S.S. Lima. IOP Conference Series: Materials Science and Engineering, 251, 2017, 012033. <https://doi.org/10.1088/1757-899x/251/1/012033>.
11. N.A. El-Hussiny, F.M. Mohamed, M.E.H. Shalabi: Science of sintering, 43, 2011, 21–31. <https://doi.org/10.2298/sos1101021e>.
12. J.M. McClelland, H. Tanaka, T. Sugiyama, T. Harada, H. Sugitatsu: Fastmet dust pellet reduction operation report on the first fastmet waste recovery plant, *In.: Iron making conference proceedings*, 2001, 629 p.
13. A. Markoti, N. Doli, V. Truji: Journal of Mining and Metallurgy, 38(3-4) B, 2002, 123–141.

<https://dx.doi.org/10.2298/JMMB0204123M>.

14. S. Fenwei, H.O. Lampinen and R. Robinson: ISIJ international, 44(4), 2004, 770–776. <https://doi.org/10.2355/isijinternational.44.770>.

15. Z. Wang, D. Pinson, Sh. Chew, B.J. Monaghan, M.I. Pownceby, N. Webster, H. Rogers, G. Zhang. Effect of addition of mill scale on sintering of iron ores. Metallurgical and Materials Transactions B, 47B, 2016, 2848–2860. <http://dx.doi.org/10.1007/s11663-016-0738-2>.

16. E.F. Wegman. *Agglomeration of ores and concentrates*. Moscow: Metallurgy, 1984, 256 p.

17. A. Zhunosova, P. Bykov, A. Zhunosov, A. Kenzhebekova: Kompleksnoe ispolzovanie mineralnogo syra = Complex Use of Mineral Resources, 329(2), 2024; 73–81. <https://doi.org/10.31643/2024/6445.19>.

18. T.Ya. Malysheva, O.A. Dolitskaya. *Petrography and mineralogy of iron ore raw materials: textbook for universities*. Moscow: MISIS, 2004, 424 p.

19. B. Kelamanov, Ye. Kyatbay, G. Yerekeyeva, T. Tushyev: Acta Metallurgica Slovaca, 30(2), 2024, 51–56.

<https://doi.org/10.36547/ams.30.2.2014>.

20. A. Nurumgaliyev, T. Zhuniskaliyev, V. Shevko, B. Kelamanov, G. Yerekeyeva, I. Volokitina: Scientific Reports, 14(1), 2024, 7456. <https://doi.org/10.1038/s41598-024-57529-6>.

21. B.A. Svyatov, M.Zh. Tolymbekov, S.O. Baisanov. *Formation and development of the manganese industry in Kazakhstan*. Almaty: Iskander, 2002, 416 p.

22. M.T. Abedghars, M. Ghers, S. Bouhouche, B. Bezzina: Bull. Min. Res. Exp. 2020 (162) 1–9. <http://bulletin.mta.gov.tr>.

23. D. Walter, G. Buxbaum, W. Laqua. J therm anal calorim, 63, 2001, 733–748. <https://doi.org/10.1023/a:1010187921227>.

24. S.U. Ofoegbu. Characterization studies on agbaja iron ore: a high-phosphorus content ore. SN Applied Science, 1(3), 204, 2019. <https://doi.org/10.1007/s42452-019-0218-9>.

25. L.B. Tolymbekova, A.S. Kim, A.K. Zhunosov, A.A. Babenko: Metallurgist, 56, 2013, 919–924.

<https://doi.org/10.1007/s11015-013-9675-3>.

26. O. Sariyev, B. Kelamanov, M. Dossekenov, A. Davletova, Ye. Kumatbay, T. Zhuniskaliyev, A. Abdirashit, M. Gasik. Heliyon, 10(9), 2024, e30789. <https://doi.org/10.1016/j.heliyon.2024.e30789>.